Supporting Information

Yamaji et al. 10.1073/pnas.1015793108

SI Materials and Methods

Primary Antibodies. Paraffin or frozen tissue sections were used for immunofluorescent and immunohistochemical staining with the following antibodies: rabbit polyclonal antibody against human β-catenin (Cell Signaling Technology), mouse monoclonal antibody against human cytokeratin 8 (gift from R. Oshima, Sanford-Burnham Medical Research Institute, La Jolla, CA), and rat monoclonal antibody against mouse E-cadherin (Zymed). Additional antibodies used in Western blot analysis are rabbit polyclonal antibodies against human c-Myc, human IκBα, and mouse IκBβ, mouse monoclonal antibodies against rat PCNA (all from Santa Cruz Biotechnology), and mouse monoclonal antibodies against human p38 and JNK (both from Cell Signaling Technology). Antibodies against Ki67, BrdU, p21, p27, c-Jun, and β-tubulin have been described in our previous studies.

Flow Cytometry Analysis of Hepatocytes. A modified hypotonic lysis method was developed for DNA content measurement and sorting of hepatocytes by flow cytometry. Briefly, isolated hepatocytes were frozen in a −80 °C freezer overnight or longer, thawed on ice, resuspended in 500 μL PI-containing hypotonic lysis buffer (0.1% Triton X-100, 50 μg/mL PI, 100 μg/mL RNase I, and 0.1% sodium citrate). After incubation on ice for 1 h with occasional gentle shaking, nearly all cells were detached in solution under phase-contrast light microscopy. These cells were then analyzed with a FACSort analyzer (Becton Dickinson). The collected data were analyzed with FlowJo software for gating correction and cell cycle profiling.

Liver cDNA Preparation and Analysis. Snap-frozen liver tissues were homogenized by a Polytron homogenizer (Brinkmann Instruments) and total RNA was isolated from the homogenates using RNeasy kit (Qiagen). Total RNA (1 μg) was treated with RNase-free DNase (Promega), and first-strand cDNA was generated with oligo(dT) primers by using a SuperScript III First Strand Synthesis Kit (Invitrogen). PCR was performed in 25-μL reactions with 5 μL diluted cDNA templates mixed with 20 μL PCR mix containing 1.25 U Taq polymerase (BioLabs). The following thermal cycle profile was used to amplify CRE and 18S rRNA: 94 °C for 20 s, 56 °C for 20 s, and 72 °C for 1 min for 40 cycles. The primers are as follows: for CRE, 5′-GCATTACCGGTCGATGCAACGAGTGATGAG-3′ and 5′-GAGTGAACGAACCTGGTCGAAATCAGTGCG-3′; and for 18s rRNA, 5′-GTAACCCGTTGAACCCCATT-3′ and 5′-CCATCCAATCGGTAGTAGCG-3′. Reaction products were separated in 1% agarose gel and imaged by using a FluorChem imager (Alpha Innotech).

Liver Function Assays. Blood samples (150 μL) collected from mice via retro-orbital bleeding were analyzed using a mammalian liver enzyme profile rotor on a VetScan VS2 analyzer. At least three animals of matching ages from each genotype were assayed.

Steatosis Staining. For steatosis assays, 10-μm frozen liver sections were incubated in 60% isopropanol for 2 min and then in freshly prepared oil red solution (0.2% oil red in 60% isopropanol) for 20 min.

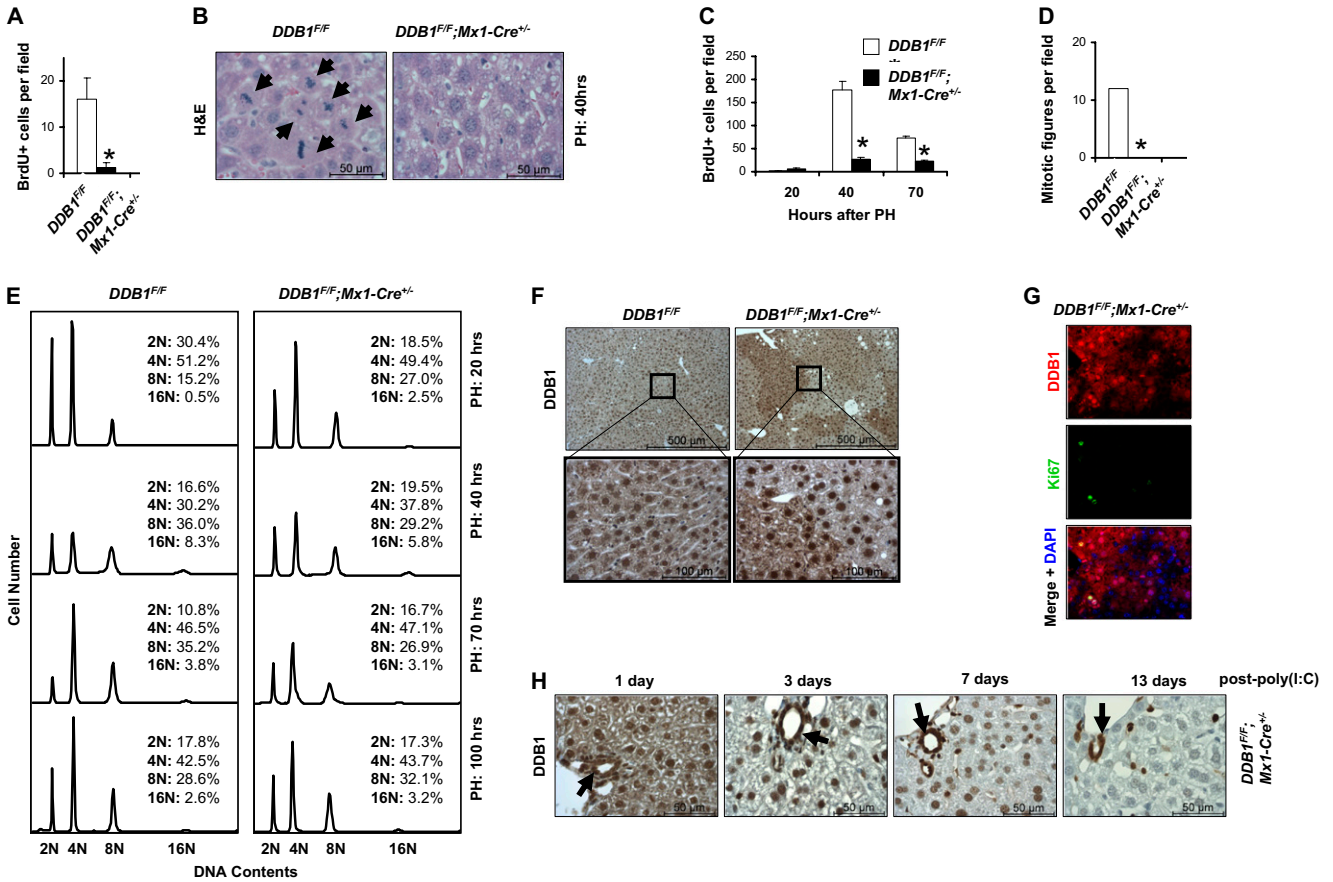

Fig. S1. Characterization of *DDB1*$^{F/F}$;*Mx1-Cre*$^{+/-}$ mice after induced deletion of DDB1 by poly(I:C) injection. (*A*) Counting of BrdU-positive hepatocytes in Fig. 1*C*. Values presented as means ± SEM (*$P < 0.01$). (*B*) Histological analysis of liver sections 40 h after PH by staining with H&E. Arrows indicate hepatocytes in mitosis. (*C*) Counting of BrdU-positive hepatocytes in Fig. 1*D*. Values presented as means ± SEM (*$P < 0.01$). (*D*) Counting of mitotic figures in *B*. Values presented as means ± SEM (*$P < 0.01$). (*E*) Flow cytometry analysis of DNA contents in hepatocytes isolated from experimental mice as in Fig. 1*D*. Percentage of cells with 2N, 4N, 8N, and 16N chromosomes was indicated within each graph. (*F*) IHC staining for DDB1 on liver sections from poly(I:C)-treated *DDB1*$^{F/F}$ or *DDB1*$^{F/F}$;*Mx1-Cre*$^{+/-}$ mice 3 mo after PH. (*G*) Co-IF staining for DDB1 and Ki67 on liver sections from a *DDB1*$^{F/F}$;*Mx1-Cre*$^{+/-}$ mouse 6 wk after poly(I:C) injection. (*H*) IHC for DDB1 on liver sections from *DDB1*$^{F/F}$;*Mx1-Cre*$^{+/-}$ mice 1, 3, 7, and 13 d after poly(I:C) injection. Arrows indicate DDB1-expressing bile duct cells as an internal staining control for the time-dependent loss of nuclear DDB1 expression in hepatocytes with deleted *DDB1* gene. It takes 10 to 14 d for DDB1 to completely disappear from the nucleus.

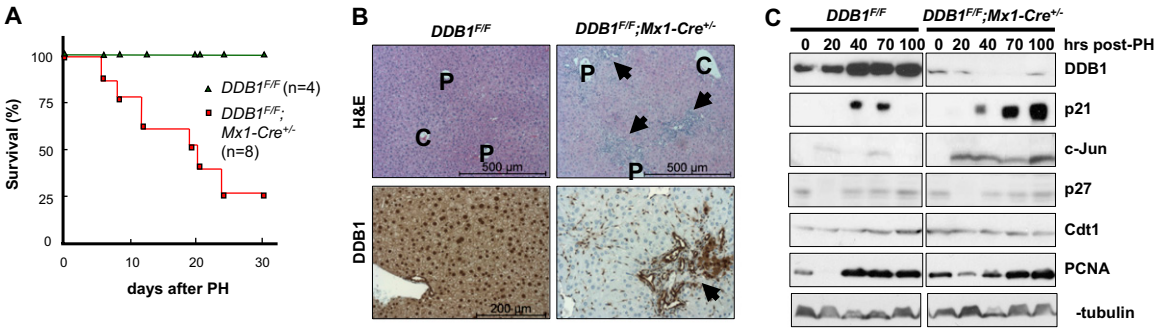

Fig. S2. DDB1-depleted liver failed to regenerate and accumulated p21 after PH. (*A*) Survival curve of poly(I:C)-treated *DDB1*$^{F/F}$ or *DDB1*$^{F/F}$;*Mx1-Cre*$^{+/-}$ mice after PH. (*B*) Histological analysis and DDB1 staining of liver sections from mice 3 wk after PH. The mutant was killed when still alive. Arrows indicate DDB1-expressing proliferating duct-like epithelial cell. Note that almost all hepatocytes are negative for DDB1. P, portal vein; C, central vein. (*C*) Western analysis of levels of the substrates of DDB1-Cul4A ubiquitin ligase in total liver lysates from mice after PH.

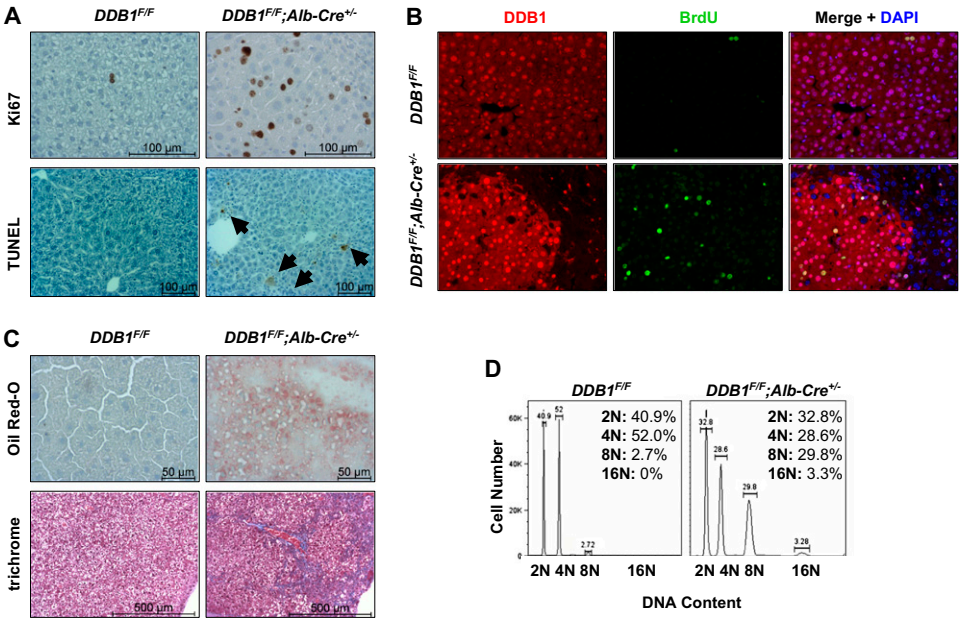

Fig. S3. Characterization of young *DDB1*$^{F/F}$;*Alb-Cre*$^{+/-}$ mice. (*A*) Ki67 staining and TUNEL analysis on liver sections from 2-mo-old mice. Arrows indicate TUNEL-positive cells. (*B*) Co-IF staining for DDB1 and BrdU on liver sections from 2-mo-old mice showing all BrdU-positive hepatocytes expressing DDB1. (*C*) Oil red O staining of frozen liver sections reveals lipid droplets, and trichrome staining of paraffin liver sections reveals mild extrahepatic collagen aggregation. (*D*) Flow cytometry analysis of DNA contents in hepatocytes isolated from adult mice.

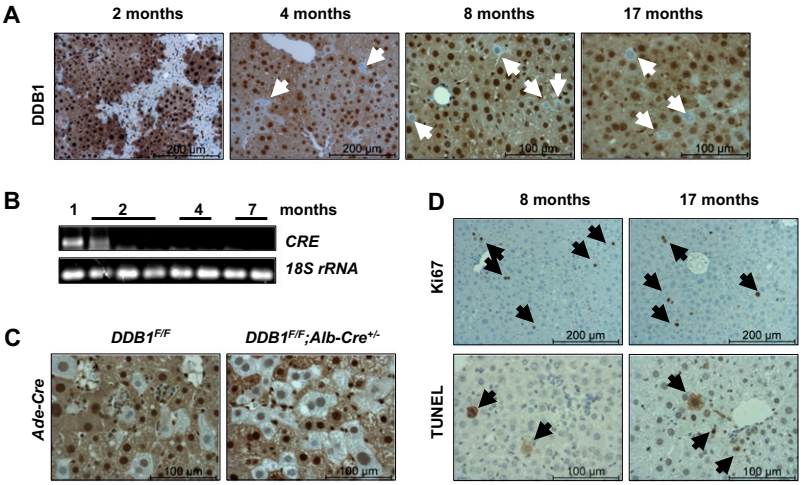

Fig. S4. Characterization of old *DDB1*$^{F/F}$;*Alb-Cre*$^{+/-}$ mice. (*A*) IHC staining for DDB1 on liver sections from 2-, 4-, 8-, and 17-mo-old old *DDB1*$^{F/F}$;*Alb-Cre*$^{+/-}$ mice. White arrows indicate DDB1-deficient hepatocytes. (*B*) PCR analysis of *CRE* cDNA levels in livers of *DDB1*$^{F/F}$;*Alb-Cre*$^{+/-}$ mice at indicated ages. (*C*) DDB1 staining on liver sections from 8-mo-old *DDB1*$^{F/F}$ or *DDB1*$^{F/F}$;*Alb-Cre*$^{+/-}$ mice 2 wk after receiving intrasplenic injection of adenoviruses expressing Cre (Ade-Cre). (*D*) Ki67 staining and TUNEL analysis on liver sections from the same mice as in *A*. Arrows indicate positively stained hepatocytes.

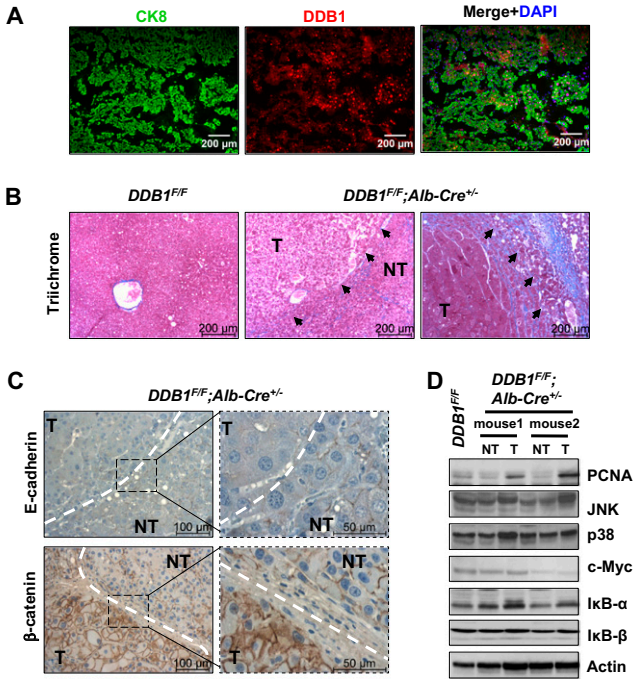

Fig. S5. Characterization of liver tumors arising from *DDB1*$^{F/F}$;*Alb-Cre*$^{+/-}$ mice. (*A*) Co-IF for cytokeratin 8 (CK8) and DDB1 on frozen tumor sections. (*B*) Trichrome staining on tumor sections from two animals. Arrows indicate tumor edges. (*C*) IHC staining for E-cadherin and β-catenin on tumor sections showing their distinct expression in tumors and nontumor tissue. (*D*) Western analysis of levels of proteins implicated liver tumorigenesis.

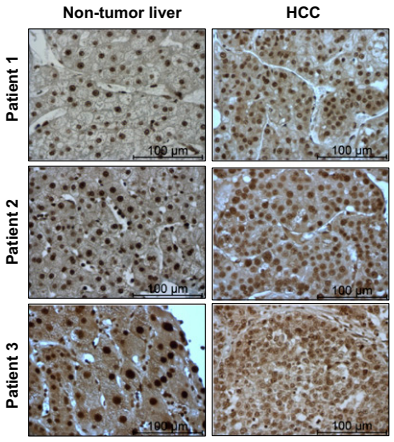

Fig. S6. No deregulation of DDB1 expression in human HCC samples. IHC staining for DDB1 on tissue sections of HCC and its neighboring nontumor liver from three patients.

Table S1. Analysis of *DDB1*$^{F/F}$;*Alb-Cre*$^{+/-}$ mice with liver tumors

	Animals with tumors/total examined (%)			
Genotypes	14–15 mo	16–17 mo	18–19 mo	20–22 mo
DDB1$^{F/F}$;*Alb- Cre*$^{+/-}$ *	0/10 (0%)	2/11 (18%)	6/17 (35%)	17/21 (81%)
DDB1$^{F/F}$ or *DDB1*$^{F/+}$	0/8 (0%)	0/14 (0%)	0/12 (0%)	1/19 (5%)
DDB1$^{F/+}$;*Alb-Cre*$^{+/-}$	—	—	0/5 (0%)	
DDB1$^{F/\Delta}$ or *DDB1*$^{+/\Delta}$	—	—	1/22 (5%)	

*Analyses also include mice with genotype *DDB1*$^{F/\Delta}$;*Alb-Cre*$^{+/-}$. *DDB1*$^{F/\Delta}$;*Alb-Cre*$^{+/-}$ mice showed no obvious difference in liver development and tumorigenesis from *DDB1*$^{F/F}$;*Alb-Cre*$^{+/-}$ mice.